Hierarchical homogenization with deep-learning-based surrogate model for rapid estimation of effective permeability from digital rocks

Mingliang Liu[1], Rasool Ahmad[2], Wei Cai[2] and **Tapan Mukerji[1]**

[1] Department of Energy Resources Engineering, Stanford University, USA.

[2] Micro and Nano Mechanics Group, Department of Mechanical Engineering, Stanford University, USA.

Corresponding author: Mingliang Liu (mliu9@stanford.edu)

Key Points:

- A large digital rock dataset is generated for use in machine learning research of permeability prediction.
- 3-D convolutional neural network is an efficient surrogate model for estimation of permeability of sub-volumes of digital rocks.
- The hierarchical homogenization method provides a computationally efficient way to predict effective permeability of large digital rocks.

Abstract

Effective permeability is a key physical property of porous media that defines its ability to transport fluid. Digital rock physics combines modern tomographic imaging techniques with advanced numerical simulations to estimate effective rock properties. Digital rock physics is used to complement or replace expensive and time-consuming or impractical laboratory measurements. However, with increase in sample size to capture multimodal and multiscale microstructures, conventional approaches based on direct numerical simulation (DNS) are becoming very computationally intensive or even infeasible. To address this computational challenge, we propose a hierarchical homogenization method (HHM) with a data-driven surrogate model based on 3-D convolutional neural network (CNN) and transfer learning to estimate effective permeability of digital rocks with large sample sizes up to billions of voxels. This workflow (HHM-CNN) divides the large digital rock into small sub-volumes and predicts the sub-volume permeabilities through a CNN surrogate model of Stokes flow at the pore scale. The effective permeability of the full digital rock is then predicted by solving the Darcy equations efficiently on the upscaled model in which the permeability of each cell is assigned by the surrogate model. The proposed method is verified on micro-CT data of both sandstones and carbonates as well as the reconstructed high-resolution digital rock obtained by multiscale data fusion. The computed permeabilities of our proposed hierarchical approach are consistent with the results of the DNS on the full digital rock. Compared with conventional DNS algorithms, the proposed hierarchical approach can largely reduce the computational time and memory demand.

Plain Language Summary

Digital rock physics has become a routine tool in characterization of porous media. As a complement to conventional core analysis by laboratory experiments that are expensive and time-consuming, digital rock physics enables us to obtain effective rock properties through the numerical simulation of physical processes with digital representation of the pore geometry obtained from high-resolution imaging. However, nowadays, the sample size of digital rock images is often up to billions of voxels. The demand for computing resources is so great that direct numerical simulation on such large-scale samples is impractical. In this study, we develop a hierarchical homogenization method with a data-driven surrogate model based on convolutional neural network to rapidly estimate effective permeability of digital rocks with large size. The predicted permeabilities of our proposed method are generally consistent with the results of conventional algorithms using direct numerical simulation and the computational time is reduced by orders of magnitude.

1. Introduction

Understanding the behavior of fluid flow through porous media is crucial for a broad range of subsurface applications such as oil and gas recovery, carbon dioxide storage, groundwater management and nuclear waste disposal. At the pore scale, the flow physics of fluids in porous rocks is governed by the spatial configuration of pores, e.g., pore shape, throat size and connectivity. At the macroscopic scale, it is referred to as effective permeability that provides a volume-averaged geometric measure to quantify the ease with which a fluid flows through a specific rock volume.

With the advancement of tomographic imaging techniques and the rapid growth of high-performance computing, digital rock physics (DRP) has gained increasing attention in pore-scale physics simulation and estimation of effective properties (e.g., permeability, formation factor and elastic moduli) (Andrä et al., 2013a and 2013b; Blunt et al., 2013; Keehm et al., 2001 and 2004; Saxena et al., 2017). The typical DRP workflow includes three steps: 1) acquiring raw digital rock data by tomographic imaging; 2) segmenting raw digital rock images to different phases and 3) calculating physical properties by numerical simulation on the segmented images (Andrä et al., 2013a and 2013b). Specifically, common numerical methods for fluid flow simulation on digital rock images include the finite difference method (e.g. Shabro et al., 2012), the finite element method (e.g. Vianna et al., 2020), the finite volume method (e.g. Raeini et al., 2012) and the lattice Boltzmann method (e.g. Keehm et al., 2004). In principle, DRP provides a non-destructive way to study porous media in a repeatable and more efficient manner as a complement to conventional laboratory measurements. Nevertheless, the computational time and memory demand of computational algorithms based on direct numerical simulation (DNS) both scale up with the sample size of digital rock (Santos et al., 2020a). Nowadays, the standard size of 3D digital rock

images can be up to 2000^3 voxels, which incurs a high computational cost and thus limits the application in practice. In addition, multiresolution data fusion techniques (e.g., Liu and Mukerji, 2022) that combine large field-of-view (but low resolution) micro-CT images with high resolution (but small field-of-view) scanning electron microscope (SEM) images can also lead to high-resolution, large (~ billion voxels) 3D simulation domains. Domain decomposition (Gropp and Keyes, 1992; Chan and Mathew, 1994) is a commonly used method in computational fluid dynamic for large-scale simulations. To obtain a problem that is computationally tractable, the domain decomposition method solves the large-scale numerical problem by splitting it into a set of small problems on subdomains, enforcing continuity between adjacent subdomains. Some attempts have been made to address the computing issue in DRP by using the technique of domain decomposition (Balhoff et al., 2007; Da Wang et al., 2019).

In recent years, a variety of machine learning methods have been proposed to speed up the numerical physics modeling and property prediction in DRP. Karimpouli and Tahmasebi (2019) used a convolutional neural network (CNN) to predict P- and S-wave velocities from 2D rock images. Cui et al. (2020) improved the prediction accuracy of velocities by adding geophysical constraints to the CNN. Santos et al. (2020) developed surrogate models based on 3D CNN for the prediction of fluid flow in 3D digital rocks. Kashefi and Mukerji (2021) proposed a point cloud neural network (PointNet) for predicting the effective permeability from digital rock images. The PointNet takes point clouds of the boundaries between solid and pore spaces as input instead of the whole volume to largely reduce memory demand of graphics processing units (GPU). Rabbani et al. (2020) present a CNN model to estimate multiple parameters of porous media, such as absolute permeability, formation factor, cementation factor, tortuosity, to name a few. The main drawback of the above data-driven models is that they are only appliable to small digital rock

images (64^3 ~ 256^3) due to the limitation of GPU memory and/or the limited number of training samples. Santos et al. (2021) proposed a multiscale CNN for the prediction of fluid flow that can handle digital rock images with large size (>512^3) presenting heterogeneities at different scales. However, the network is trained with a few 256^3 samples consisting of sphere packs. Such small training set might cause the trained network difficult to be generalized to samples in real applications. Moreover, the computing time to generate enough training samples with large size can be quite long even on supercomputer clusters.

To overcome the computing challenges, hierarchical homogenization methods (HHM) are developed to estimate effective properties (e.g., permeability and elastic moduli) of large digital rocks. In the HHM, a large digital rock is divided into a set of smaller sub-volumes and the effective property of each sub-volume is obtained by DNS or data-driven methods. The effective property of the full rock volume is then computed by numerical simulation on the upscaled rock with fewer degrees of freedom than the original digital rock. Menke et al. (2020) proposed an HHM for estimation of effective permeability in which the permeabilities of sub-volumes are predicted by an Extra-Trees regression model. However, there exists several limitations of their approach: 1) Only averaged geometric attributes (e.g., porosity, phase connectivity and volume fractions) are used by the regression tree model to predict the permeability of sub-volumes. The loss of local structure information might lead to inaccurate prediction; 2) The machine learning model is trained and validated on the same rock sample. It is hard to guarantee the generalization capability of the model; 3) The Brinkman-Stokes model is used to predict permeabilities of sub-volumes for the generation of training set. This requires the porosity and permeability of each voxel, which are usually not readily available in practice. It also ignores the actual high-resolution information represented by voxels of pore or mineral (binary), and the flow physics at that scale

which is Stokes flow not the Stokes-Brinkman flow. Ahmad et al. (2022) applied the HHM to compute elastic moduli of large digital rocks and systematically analyzed the error arising due to HHM. Instead of data-driven methods, they used a fast Fourier transform (FFT) based elasticity solver to obtain the effective moduli of sub-volumes which is more accurate and robust but at the expense of computing cost.

Inspired by the works of Menke et al. (2020) and Ahmad et al. (2022), we apply the HHM for rapid estimation of effective permeability of large digital rocks with a surrogate model based on 3-D CNN and transfer learning to address the above issues. The main contributions of our paper are as follows:

1) We use CNN as the surrogate model to quickly and accurately predict permeability of sub-volumes that can exploit both global and local information of microstructures.
2) To make sure that the CNN model has a good generalization capacity, we create two large training data sets for both sandstones and carbonates. The permeabilities of training samples are computed by solving the Stokes equations on binary (solid and pore phase) 3-D images, which does not require the porosity and permeability of each pixel. To the best of our knowledge, they are the largest training sets for permeability estimation in DRP. The datasets have been made available at http://dx.doi.org/10.17632/nv5dhfj86t.1.
3) We use transfer learning to solve the issue of generalization to new samples coming from a different distribution and resolution from the training set.

2. Methods

The proposed method (HHM-CNN) for computing effective permeability of large-volume digital rocks is a hierarchical approach. As illustrated in Figure 1, the workflow consists of four

steps: first, divide the full volume of digital rock into sub-volumes; second, rapidly predict the permeability of each sub-volume using a CNN surrogate model with transfer learning; third, assemble the upscaled rock model by assigning the predicted permeabilities of sub-volumes to the corresponding cells; lastly, compute the effective permeability by solving the Darcy equations on the upscaled rock model. In this study, the sub-volume size is set to 100×100×100 that is large enough to capture the correlation length of the digital rock images used in the study, and also allows us to generate a large number of training data with permeability obtained through DNS to train the CNN surrogate model.

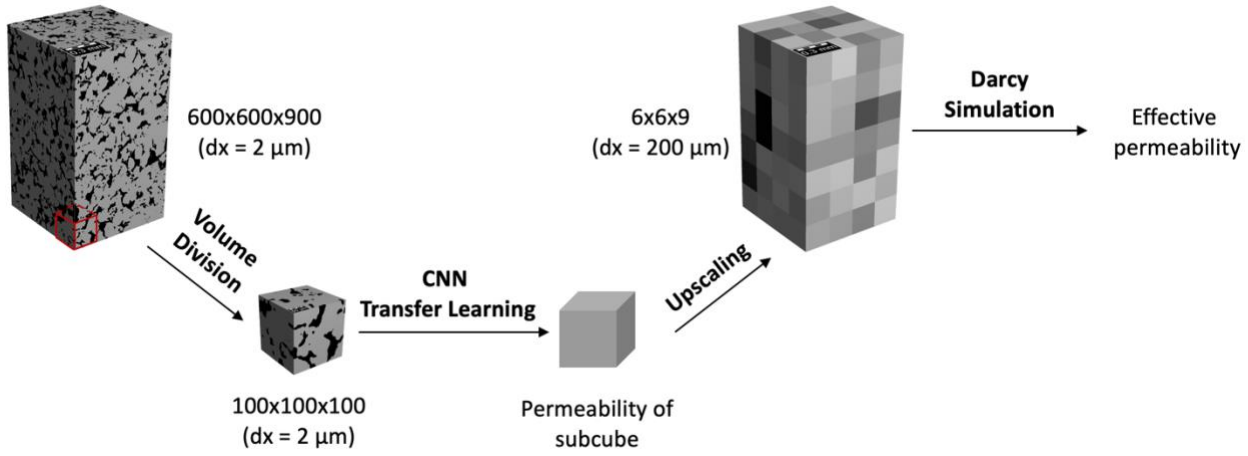

Figure 1. Workflow of HHM-CNN for estimation of effective permeability of large-volume digital rocks.

2.1 CNN with transfer learning for permeability prediction of sub-volumes

The surrogate model for rapid permeability prediction of sub-volumes is a 3D CNN, which is modified from the VGGNet (Simonyan and Zisserman, 2014). The network includes two components: feature extractor and regressor. As illustrated in Figure 2, the feature extractor consists of six convolutional blocks which extract the salient feature representation that is most

sensitive to permeability from the input binary sub-volumes. Each convolutional block includes two convolutional layers followed by a max-pooling layer. The regressor consists of three fully-connected layers that predict the logarithm of permeability ($\log k$) from the extracted features. In the inference stage with transfer learning, we freeze the feature extractor of the pre-trained CNN and fine-tune the regressor using a small number of labeled data from new digital rocks. The detailed network parameters and activation functions are listed in Table 1. The loss function is defined as the mean square error (MSE)

$$\mathcal{L} = \frac{1}{N}\sum_{i=1}^{N}(\log k_i - \log k_i')^2, \qquad (1)$$

where N is the number of training samples, $\log k_i$ is the logarithm of the permeability obtained by DNS of the ith training sample and $\log k_i'$ is the value predicted by the CNN surrogate model.

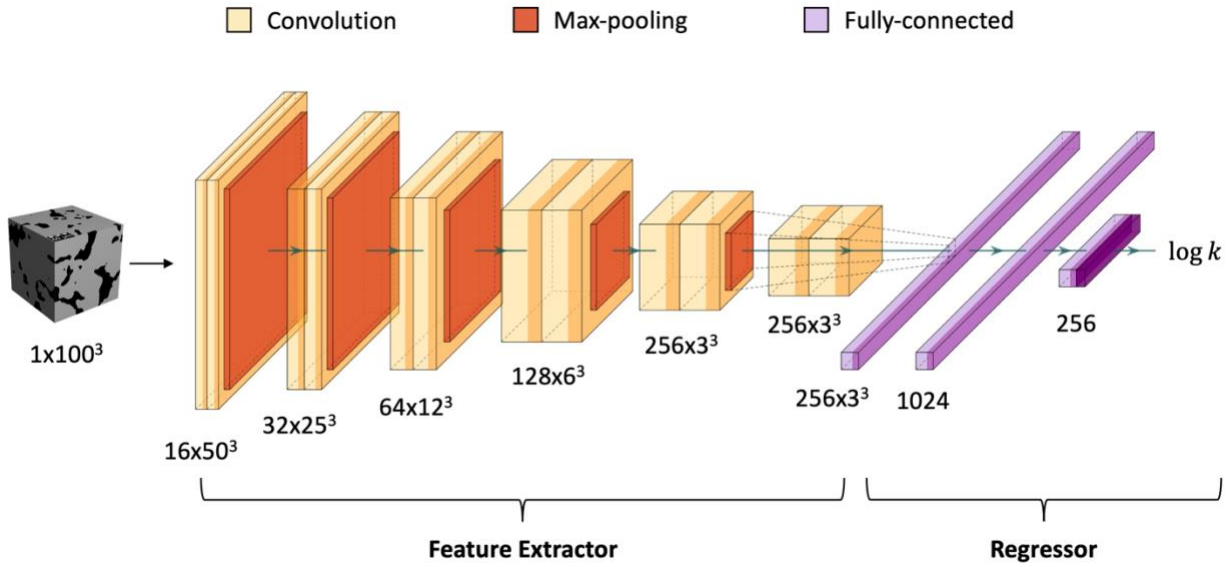

Figure 2. Architecture of the surrogate CNN model for prediction of permeability from sub-volumes with size 100^3.

Table 1. Parameters of each layer in the surrogate CNN model.

Layer	Kernel	Options	Output size
1. Input	-	-	1×100×100×100
2. Convolutional	3×3×3	Batch normalization + ReLU	16×100×100×100
3. Convolutional	3×3×3	Batch normalization + ReLU	16×100×100×100
4. Max-pooling	2×2×2	-	16×50×50×50
5. Convolutional	3×3×3	Batch normalization + ReLU	32×50×50×50
6. Convolutional	3×3×3	Batch normalization + ReLU	32×50×50×50
7. Max-pooling	2×2×2	-	32×25×25×25
8. Convolutional	3×3×3	Batch normalization + ReLU	64×25×25×25
9. Convolutional	3×3×3	Batch normalization + ReLU	64×25×25×25
10. Max-pooling	2×2×2	-	64×12×12×12
11. Convolutional	3×3×3	Batch normalization + ReLU	128×12×12×12
12. Convolutional	3×3×3	Batch normalization + ReLU	128×12×12×12
13. Max-pooling	2×2×2	-	128×6×6×6
14. Convolutional	3×3×3	Batch normalization + ReLU	256×6×6×6
15. Convolutional	3×3×3	Batch normalization + ReLU	256×6×6×6
16. Max-pooling	2×2×2	-	256×3×3×3
17. Convolutional	3×3×3	Batch normalization + ReLU	256×3×3×3
18. Convolutional	3×3×3	Batch normalization + ReLU	256×3×3×3
19. Fully-connected	-	Leaky ReLU	1024
20. Fully-connected	-	Leaky ReLU	256
21. Fully-connected	-	-	1

2.2 Generating the training dataset

Considering that microstructures (e.g., heterogeneity, pore size and pore type) of porous media vary with rock types, we train different CNN surrogate models for sandstones and carbonates with two sets of micro-CT data. The sandstone dataset includes eight samples collected from public datasets (Neumann et al., 2020) and four from our own collection. The micro-CT scanning images of the sandstone samples are shown in Figure 3. The carbonate dataset includes six limestone and dolomite samples collected from public datasets (Andrä et al., 2013a; Bultreys, 2019; Alqahtani et al., 2021) and six samples from our own collection. The micro-CT scanning images of the carbonate samples are shown in Figure 4. The selected rock samples allow us to extract sub-volumes with various kinds of pores structures (low to high porosity, small to large pores, angular to rounded, etc). The detailed information (geologic formation, size, resolution, porosity and permeability) of the sandstone and carbonate samples are available in Appendix A.

The training set with labels is one of the key factors in building data-driven algorithms of supervised deep learning. To increase the generalization capability of the CNN surrogate models, we create two large datasets of sandstone (101,348 subcubes of size 100^3 voxels) and carbonate (77,162 subcubes of size 100^3 voxels) with permeability obtained through DNS. They are randomly split into the training and validation set with a ratio of 9:1. The permeability (i.e., the label) of each sub-volume is computed by numerically solving the Stokes equations, given as

$$-\nabla p + \mu \nabla^2 \mathbf{u} = 0, \quad (2)$$

$$\nabla \cdot \mathbf{u} = 0, \quad (3)$$

where $\mathbf{u}$ is the vector field of fluid velocity, p is the scalar field of pressure and μ is the fluid viscosity. With the obtained fields of velocity and pressure, the effective permeability can be computed by Darcy's law

$$k = \mu\langle\mathbf{u}\rangle\left(\frac{\delta p}{\mathrm{L}}\right)^{-1}, \quad (4)$$

where $\langle\mathbf{u}\rangle$ is the averaged velocity vector, δp is the pressure drop in the flow direction of interest and L is the corresponding physical length of the computational domain. In this study, we focus on the fluid flow in the z direction. A low pressure drop in the z direction ($\delta p = p_{\mathrm{in}} - p_{\mathrm{out}} = 0.02$ Pa where p_{in} and p_{out} are the inlet and outlet pressure, respectively) is applied to stimulate Stokes flow in the porous media with no slip condition at the pore-solid surface ($\mathbf{u}|_{\partial V} = 0$ where ∂V is the interface between the pore and the solid phase).

We use the poreFoam package (https://github.com/ImperialCollegeLondon/poreFoam-singlePhase) to run the Stokes flow simulation on binary sub-volumes. Considering that the resolutions (voxel length) of micro-CT data vary with rock samples, the predicted permeabilities of all sub-volumes are scaled to the values at resolution of 1.0 μm (i.e., $k = k/dx^2$ where dx is the voxel length). Figure 5 shows the cross-plots between the porosity and numerically solved permeability of the sub-volumes as well as the histograms of porosity (ϕ) and $\log k$. The distributions of training and validation set are consistent. The Kozeny–Carman equations are fit to the training samples, which are $k = 4.85 \times 10^{-12}(\frac{\phi}{1-\phi})^{2.84}$ and $k = 3.82 \times 10^{-12}(\frac{\phi}{1-\phi})^{2.45}$ for the sandstone and carbonate, respectively. As shown in Figure 5, the Kozeny–Carman equations cannot capture the microstructures inherent to porous media where permeabilities range over several orders of magnitude at the same porosity.

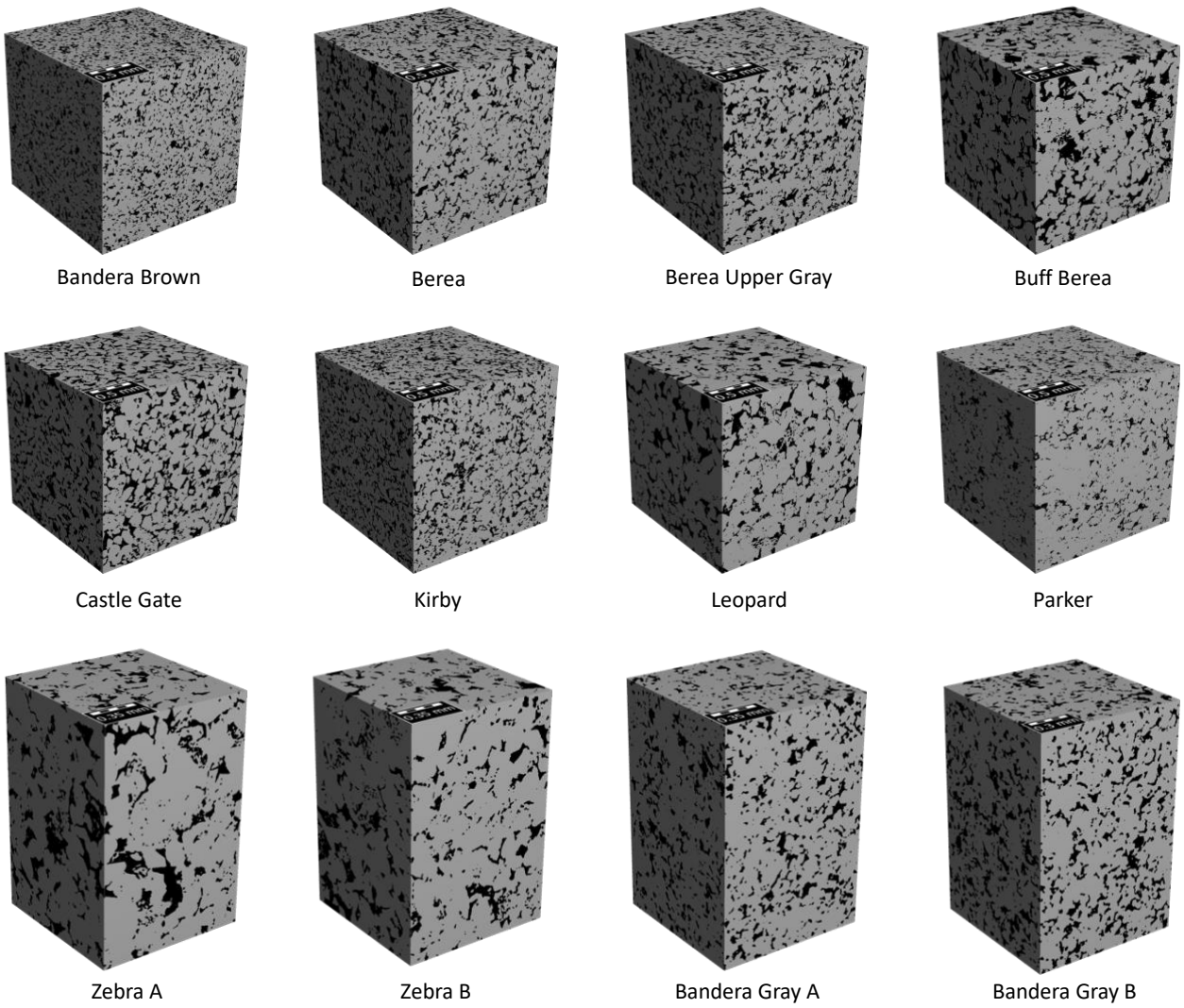

Figure 3. Micro-CT scanning images of the sandstone samples.

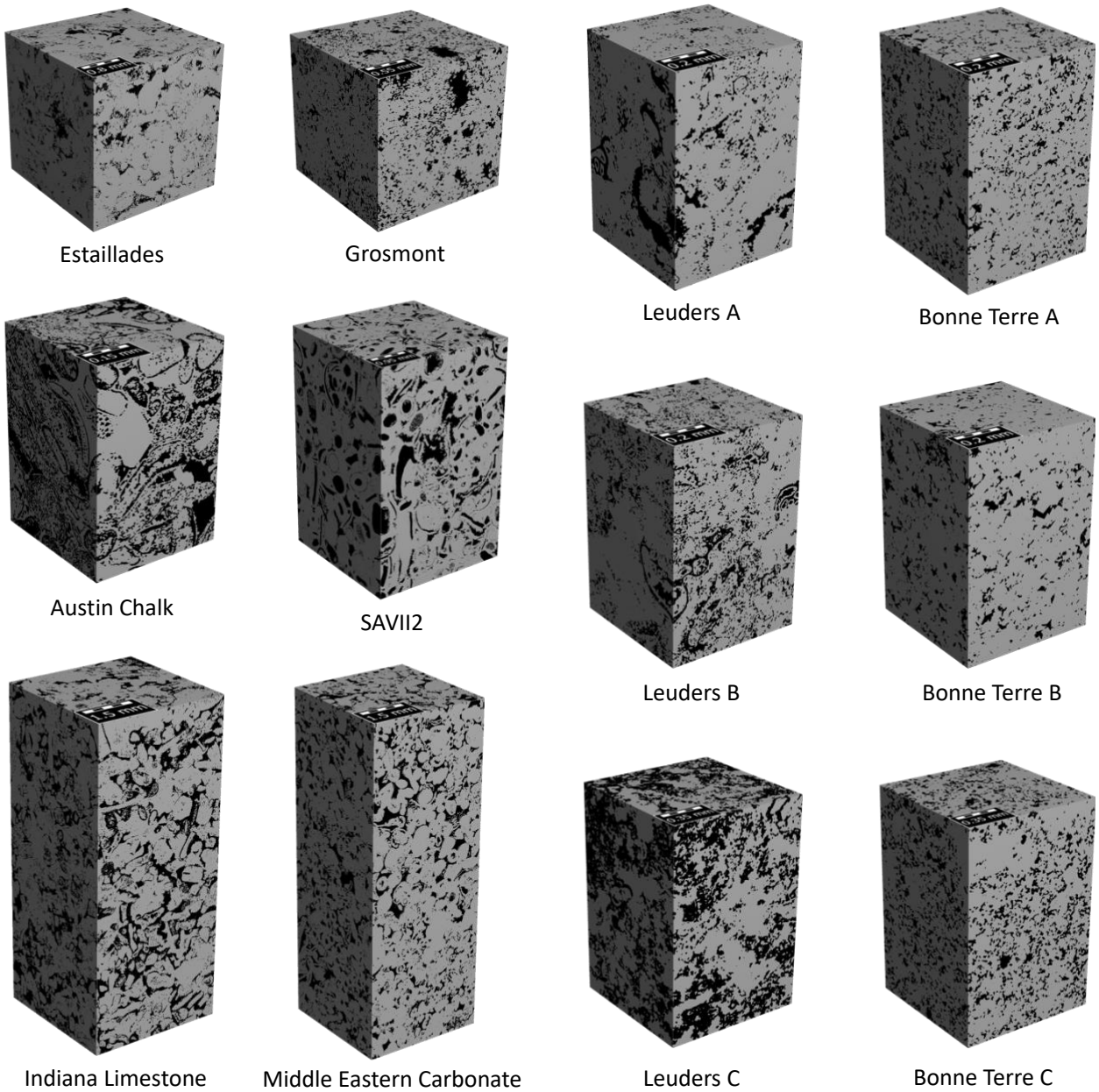

218

219 **Figure 4.** Micro-CT scanning images of the carbonate samples.

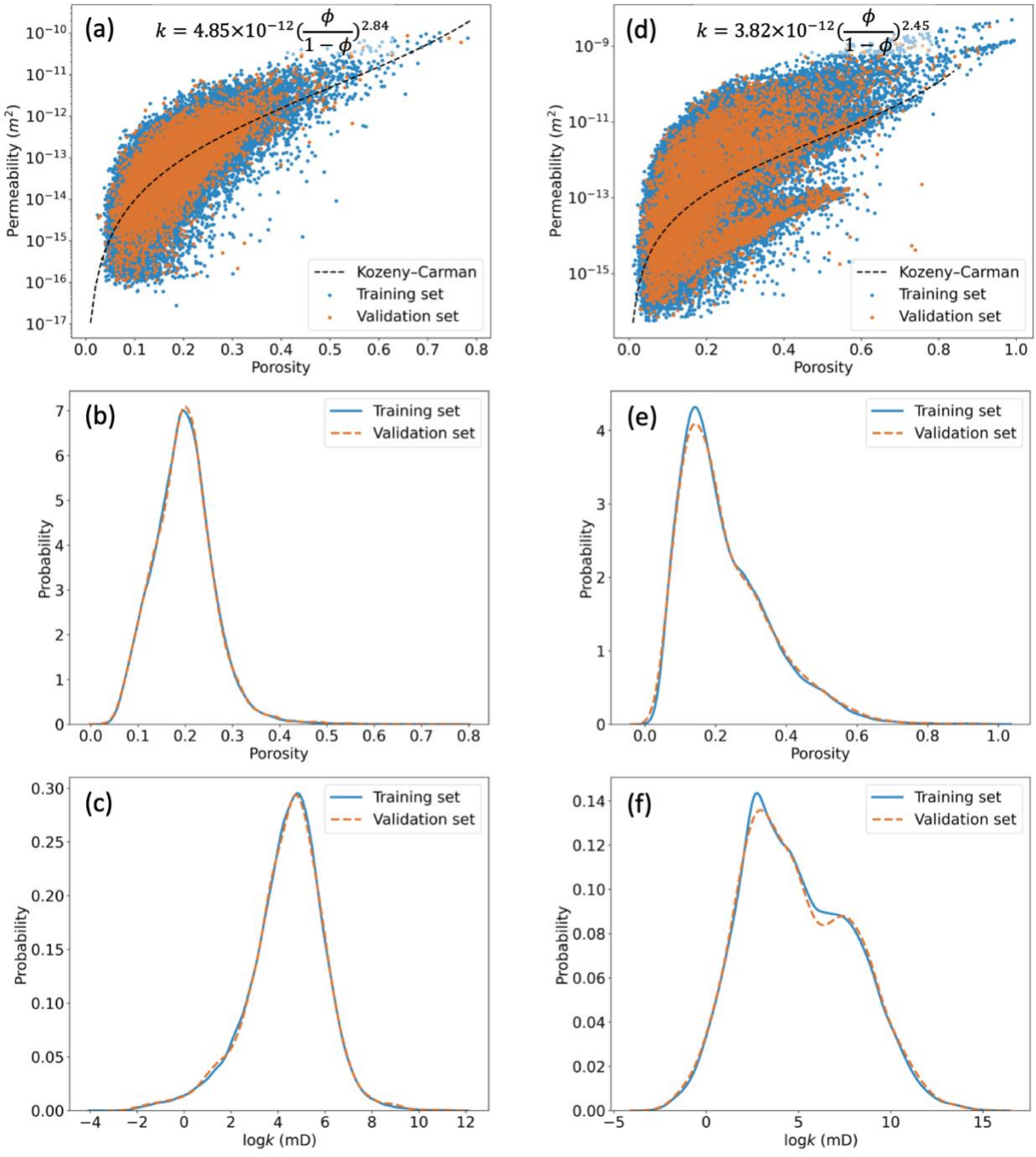

220

221 **Figure 5.** Cross-plots between porosity and permeability and histograms of the porosity logarithm of

222 permeability: (a) - (c) sandstone; (d) - (f) carbonate.

223

2.3 Effective permeability of the upscaled volumes by Darcy simulation

With the trained CNN surrogate model, we can rapidly predict the permeability of sub-volumes extracted from the digital rock images. The upscaled rock volume is assembled by assigning grid cells with the predicted permeability of corresponding sub-volumes. Then, the effective permeability of the full digital rock is computed by solving the Darcy equations

$$-\nabla p - \mu \mathbf{K}^{-1}\mathbf{u} = 0, \quad (5)$$

$$\nabla \cdot \mathbf{u} = 0, \quad (6)$$

where **K** is the permeability tensor of the upscaled cells. Here, we assume the permeability tensor is isotropic. Since the number of voxels of the upscaled rock model (from hundreds to thousands of voxels) is much less than the full digital rock (up to billions of voxels), it is computationally efficient to run the simulation of the Darcy flow on the upscaled rock.

3. Training and performance of the CNN surrogate models

The CNN surrogate models for both sandstone and carbonate are trained with a batch size of 32 and the Adam optimizer (Kingma and Ba, 2014). The learning curves of 50 iterations are shown in Figure 6. As we can see, the training loss and validation loss are close to each other with the validation loss being slightly greater than the training loss indicating no overfitting. We select the saved networks at epoch 30 where the MSE losses of both CNNs converge as the optimal models for the following evaluation.

Figure 7 shows the prediction accuracy of the CNN surrogate models. The predicted permeabilities of sub-volumes in the validation set by the CNNs are consistent with the results from DNS for both sandstone (Figure 7a) and carbonate (Figure 7c). The coefficients of

determination (R^2 score) are up to 0.98 and 0.97, respectively. The errors between the predicted and true permeabilities are approximately Gaussian with zero mean and small variances, as shown in Figure 7b and 7d. Since carbonate rocks have much more complex microstructures than sandstones, the prediction error of carbonate is slightly larger than that of sandstone. The prediction errors of the CNN surrogate model are much smaller than those from a simple Kozeny-Carman relation (Figure 7b and 7d).

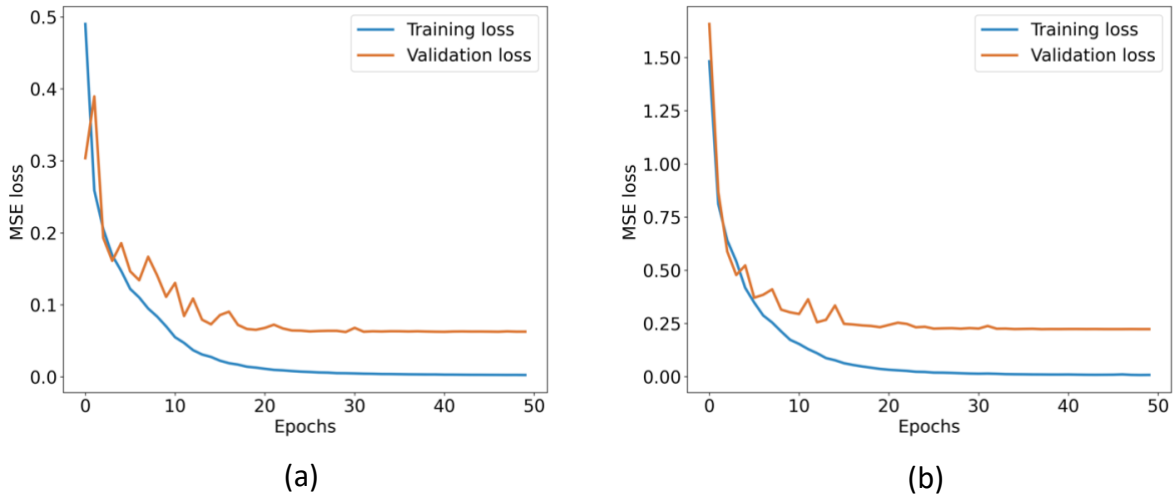

Figure 6. Training history of the CNN surrogate models: (a) sandstone; (b) carbonate.

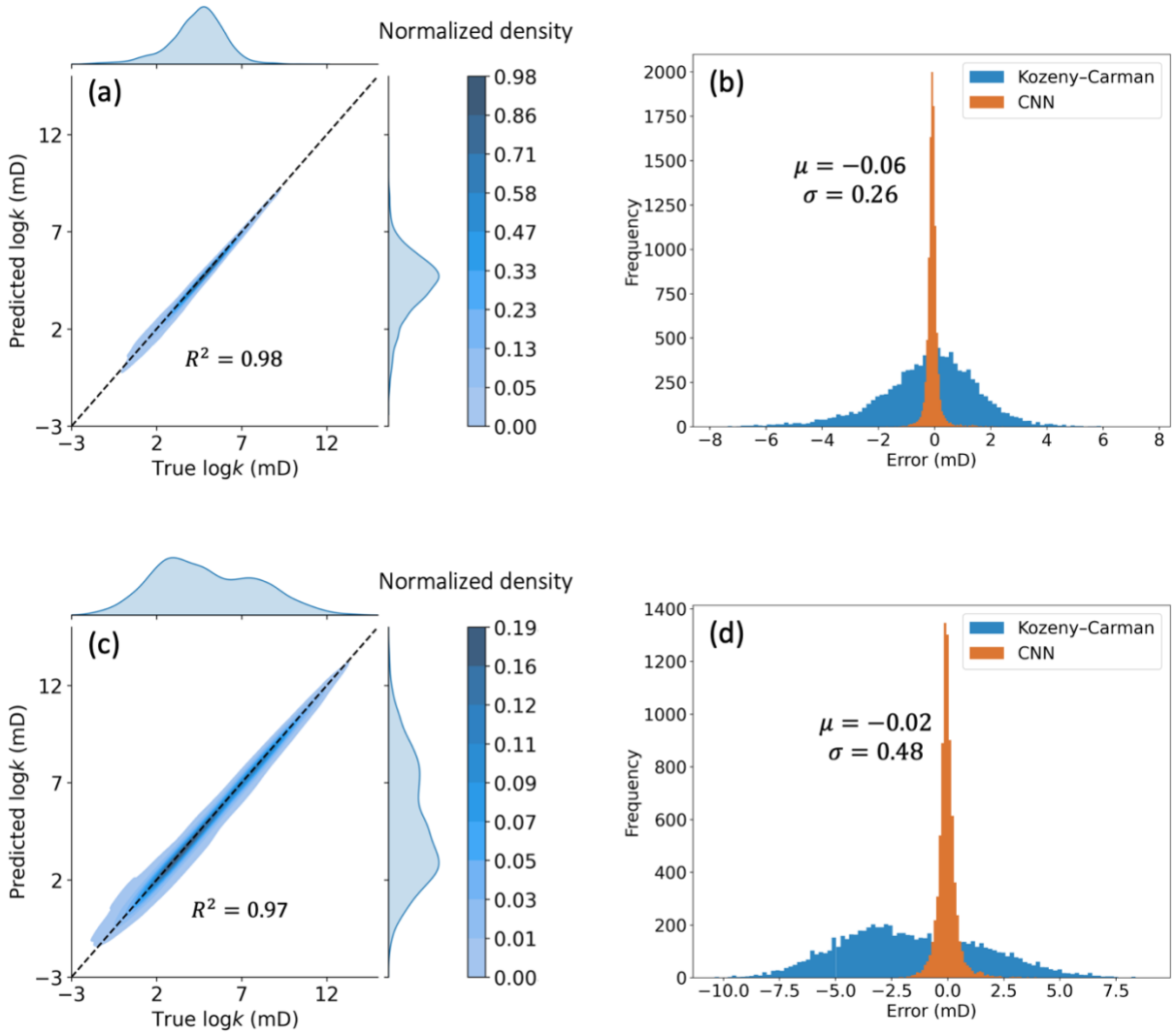

Figure 7. Prediction performance of the CNN surrogate models: (a) and (b) sandstone; (c) and (d) carbonate.

4. Results

In this section, we present the applications of HHM-CNN to predict effective permeability from large digital rock images and compare the performance with three different scenarios:

a) brute-force full DNS on the large volume,

b) HHM with DNS for the permeability prediction of sub-volumes (HHM-DNS) and

c) HHM with the Kozeny-Carman model for the permeability prediction of sub-volumes (HHM-KC).

The test rock samples are shown in Figure 8, including three sandstones (Nugget, Williams Fork and Bentheimer sandstone) and two carbonates (Edwards Brown and Desert Pink carbonate) from different formations than the ones in the training samples as well as a reconstructed high-resolution digital rock with a large size obtained by multiscale data fusion (MultiscaleDRP carbonate) (Liu and Mukerji, 2022). Nugget sandstone is a highly heterogenous rock with intermediate permeability from the Upper Triassic geologic formation in the western of United States that consists of grainflow and wind-ripple cross-strata (Lindquist, 1988). Williams Fork sandstone is a heterogeneous rock with intermediate permeability from the Upper Cretaceous geologic formation in Colorado that consists dominantly of strata deposited by fluvial systems with minor marine influences (Pranter and Sommer, 2011). Desert Pink carbonate is a homogeneous rock with high porosity and low permeability from the Edwards Plateau in Texas (Nath et al., 2017). Edwards Brown carbonate is a heterogenous rock with high porosity and high permeability also from the Edwards Plateau in Texas (Nath et al., 2017). The micro-CT volumes of the above four rock samples (i.e., Nugget, Williams Fork, Edwards Brown and Desert Pink carbonate) are all 600×600×900 (~325 million voxels) with the imaging resolution of 2.0 μm, 1.98 μm, 2.03 μm and 1.03 μm, respectively. Their computed porosities are 13%, 15%, 41% and 26%, respectively. Bentheimer sandstone is a homogeneous rock with both high porosity and permeability from a shallow marine formation deposited during the Lower Cretaceous. The micro-CT volume of the Bentheimer sandstone is 1200×1200×5000 (~7.2 billion voxels) with a resolution of 1.65 μm (Huang et al., 2021) and a computed porosity of 23%. The MultiscaleDRP

carbonate is reconstructed by integrating micro-CT data and SEM images of the Leuders carbonate. The reconstructed digital rock is 1700×1700×2600 (~7.5 billion voxels) with a resolution of 0.1 μm and a porosity of 17%.

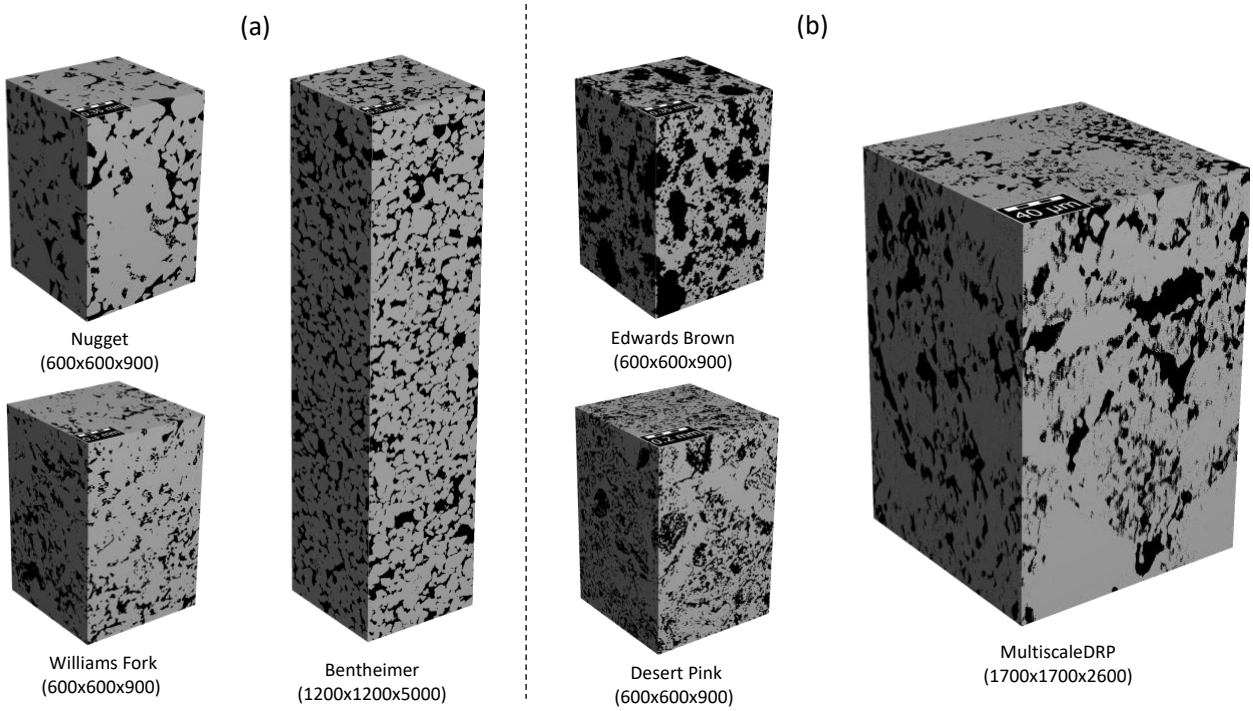

Figure 8. Test samples: (a) sandstone; (b) carbonate.

As illustrated in Figure 1, the proposed method of HHM-CNN divides the full micro-CT volumes into a set of 100^3 sub-volumes and predicts their permeabilities by the CNN surrogate model. To overcome the generalization problem that is common in data-driven methods based on supervised deep learning, for each rock sample, we randomly select 10% of the sub-volumes and compute their permeabilities through DNS using the Left-Identity-Right (LIR) solver (for solving the stationary Stokes equation) of the GeoDict software (Linden et al., 2015) for transfer learning of the pre-trained CNNs. As shown in Figure 9, the predicted permeabilities of the sub-volumes by the CNN model with transfer learning are consistent with the ground truth from the DNS using

297 the GeoDict software. The R^2 scores of the three sandstone samples and the MultiscaleDRP
298 carbonate are close to 0.9. The microstructures underlying carbonate samples are usually complex
299 and hard to be captured by the CNN. Pore structures of the Edwards Brown and Desert Pink
300 carbonate are quite different with those of the training samples. As a result, the prediction errors
301 are relatively large for the two carbonate samples with the R^2 scores of 0.76 and 0.81, respectively.

302 Figure 10 shows the predicted effective permeabilities of the full digital volumes of the test
303 samples by the four different methods: a) HHM-CNN, b) full DNS, c) HHM-DNS and d) HHM-
304 KC. The prediction uncertainty of the HHM-CNN is obtained by sampling the distributions of
305 prediction error shown in Figure 7b and 7d (for each upscaled rock realizations, we assume that
306 the errors of all sub-volumes are the same). The effective permeabilities predicted by the HHM-
307 CNN are close to the values by the HHM-DNS for all samples except the Nugget sandstone, and
308 also have a good agreement with the results from full DNS. All effective permeabilities predicted
309 by the full DNS fall in the one-sigma interval except the Williams Fork sandstone which is in the
310 two-sigma interval. The HHM-KC method is the worst in the prediction of effective permeability.

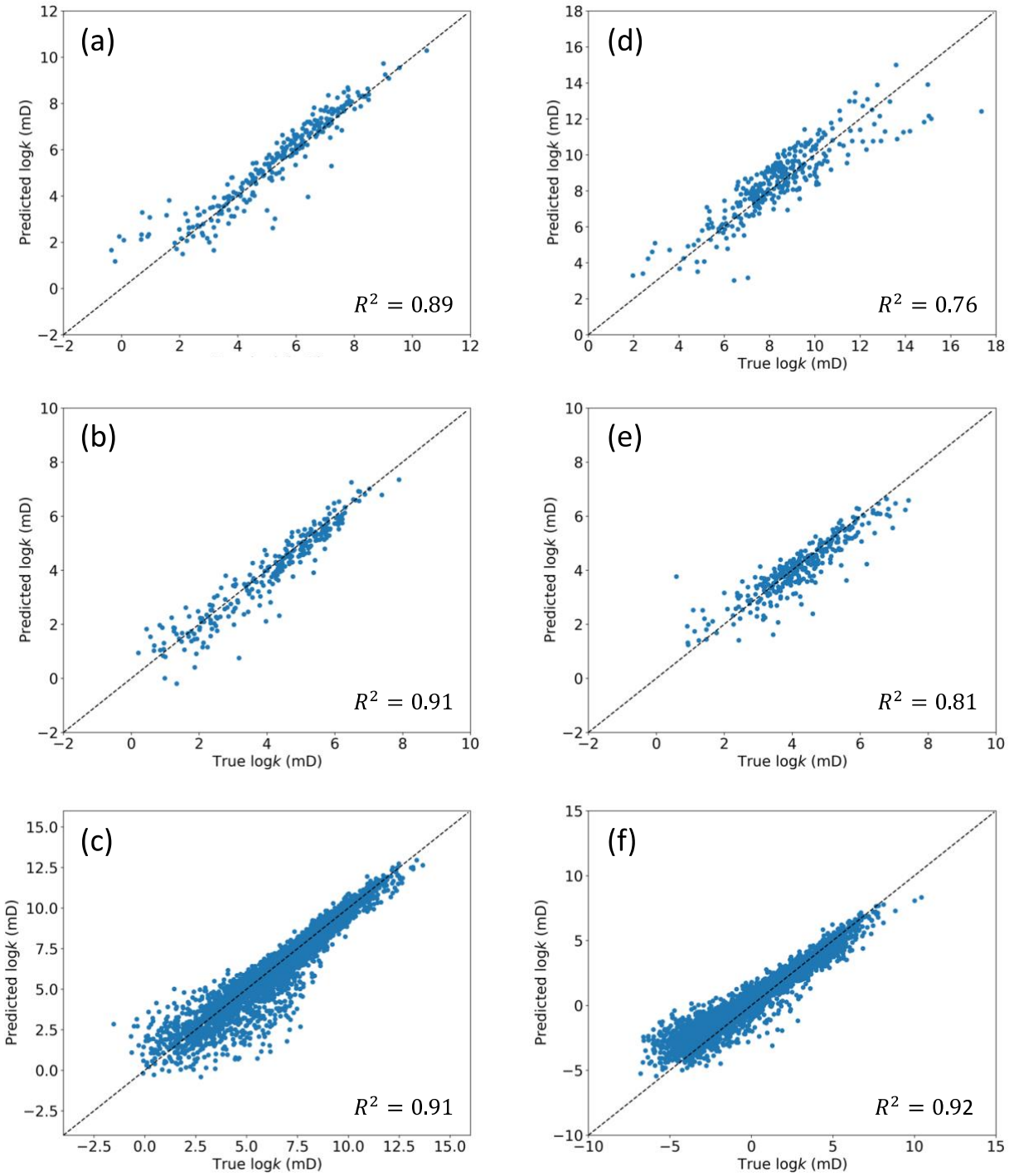

311

312 **Figure 9.** Scatter plots of the predicted permeability of sub-volumes by the CNN and DNS: (a) Nugget
313 sandstone; (b) Williams Fork sandstone; (c) Bentheimer sandstone; (d) Edwards Brown carbonate; (e)
314 Desert Pink carbonate; (f) carbonate reconstructed by multiscale data fusion.

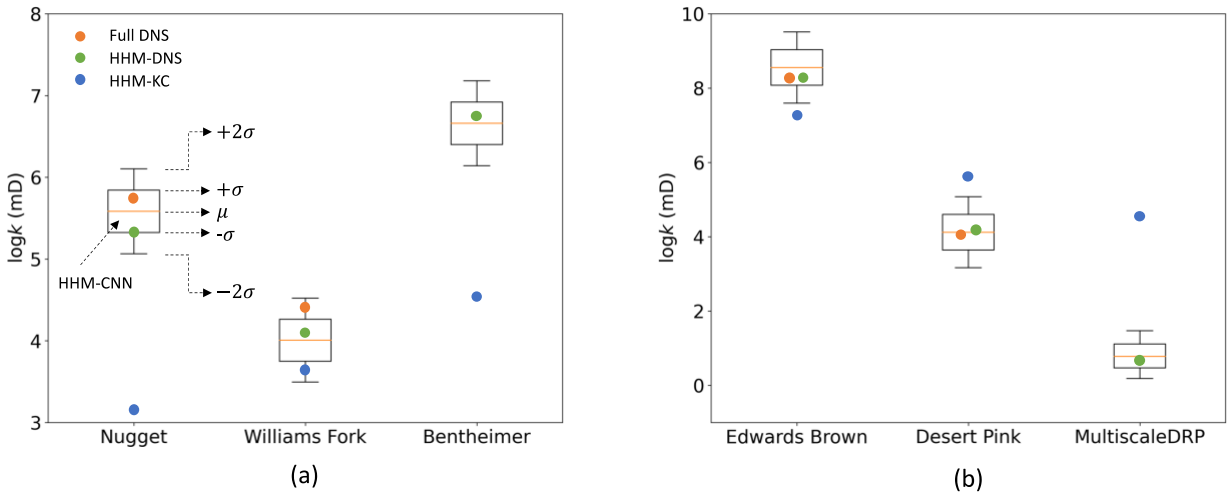

315

316 **Figure 10.** Comparison of the predicted permeabilities of the full rock volume by HHM-CNN, full DNS,
317 HHM-DNS and HHM-KC: (a) sandstone; (b) carbonate. The numbers of voxels for the Bentheimer
318 sandstone and MultiscaleDRP carbonate are up to several billions, and it is computationally impossible to
319 perform full DNS on these two large digital rocks.

320 The main advantage of the proposed hierarchical approach is that it provides a computationally
321 efficient way for rapid estimation of permeability from large digital rocks by slightly sacrificing
322 the prediction accuracy. The computational time for computing the permeabilities of the above
323 digital rocks by the full DNS, HHM-DNS and HHM-CNN are given in Table 2. The LIR solver
324 of the GeoDict software is a state-of-the-art algorithm to solve the stationary Stokes equations on
325 very large voxel geometries (Linden et al., 2015). The LIR-tree (a generalization of the Octree and
326 KD-tree) is used as an adaptive data structure for spatial partitioning, which uses coarse meshes in
327 areas with small velocity change while keeping the original resolution near the solid surfaces. The
328 adaptive meshing is helpful to speed-up the flow simulation over digital rocks with high porosity
329 and large pores. As we can see from Figure 8, the Nugget sandstone and Desert Pink carbonate are
330 dominated by large pores. Although they have the same voxel size (600×600×900) as the Williams
331 Fork sandstone and Edwards Brown Carbonate, their computational times for full DNS with the

LIR solver are much smaller. The computational time of the HHM-DNS with sub-volume size 100^3 is slightly reduced for the Nugget sandstone but reduced by about three times for other three 600×600×900 samples. Our proposed method of HHM-CNN can further reduce the computational time to several minutes using one Nvidia A100 GPU. The numbers of voxels of the Bentheimer sandstone and MultiscaleDRP carbonate are up to several billions. It is computationally impossible to perform full DNS on such large digital rocks. It takes about 4.5 hours to compute their effective permeabilities with the HHM-DNS, while it takes about 20 minutes with the HHM-CNN. The corresponding speed-up ratios are about 10.

Table 2. Computational time (seconds) of full DNS, HHM-DNS and HHM-CNN.

	Full DNS (GeoDict – 16 cores)	**HHM-DNS (GeoDict – 16 cores)**	**HHM-CNN (A100 GPU)**
Nugget Sandstone	1260	1008	201
Williams Fork Sandstone	4968	1571	263
Bentheimer Sandstone	-	15814	1361
Desert Pink Carbonate	2836	980	94
Edwards Brown Carbonate	6084	1739	180
MultiscaleDRP Carbonate	-	15434	1426

5. Discussions

The proposed hierarchical approach for upscaling of digital rocks is a hybrid physics and data-driven method. Its advantage in computational efficiency comes from two aspects. First, fluid flow

simulations on sub-volumes with small size are much easier and faster to solve numerically than the full volume that involves solving a large (up to billions) system of linear equations. Secondly, the data-driven surrogate models based on CNNs enable predicting permeability of sub-volumes almost instantly. However, on the other hand, the hierarchical approach will introduce additional modeling errors and thus reduce the accuracy of estimation to some extent (Ahmad et al., 2022). In this study, we assume the permeabilities of sub-volumes are isotropic. This simplification is helpful to reduce the computational costs of preparing labeled samples for the training of CNNs because it is only necessary to run the flow simulation along one direction. To improve the prediction accuracy, it would be better to use an anisotropic permeability tensor instead. In addition, we adopt the CNNs modified from the VGGNet as the surrogate model in this study. Many other deep neural networks, such as Residual neural network (ResNet) (He et al., 2016) and Vision in Transformer (ViT) (Dosovitskiy et al., 2020) might be useful to improve the performance of the surrogate models. Although we focus on the flow property of permeability in this paper, it is straightforward to extend the hierarchical homogenization approach for estimation of other petrophysical properties, such as elastic moduli and electric resistivity.

6. Conclusions

We developed a hierarchical homogenization approach for rapid prediction of effective permeability from large digital rocks, which is a hybrid algorithm of data-driven surrogate model and numerical physics. The applications to real sandstone and carbonate micro-CT data as well as a digital rock with extremely large size obtained by multiscale data fusion reveals that the proposed hierarchical method is a valid and computationally efficient approach for estimation of effective

permeability. The data-driven surrogate models based on 3-D CNNs are trained with a large number of training samples with permeabilities obtained by pore-scale direct numerical solution (DNS) of fluid flow and enable rapid estimation of permeabilities of 100^3 sub-volumes having a good generalization capacity with transfer learning. The effective permeabilities numerically computed by Darcy flow simulation on the upscaled models are consistent with the results obtained by DNS on the full digital rocks. Moreover, compared with conventional methods based on DNS, the proposed hierarchical approach greatly reduces the computational time and memory requirement.

Appendix A: Information of sandstone and carbonate rocks

The detailed information of sandstone and carbonate rocks used in this study are listed in Table 3 and Table 4, respectively.

Table 3. Information of sandstone rocks.

No.	Name	Formation	Size	Resolution (μm)	Porosity	Permeability
1	Bandera Brown	Upper Carboniferous	1000×1000×1000	2.25	0.17	Low
2	Berea	Upper Devonian	1000×1000×1000	2.25	0.22	Intermediate
3	Berea Upper Gray	Upper Devonian	1000×1000×1000	2.25	0.20	Intermediate
4	Buff Berea	Upper Devonian	1000×1000×1000	2.25	0.23	Intermediate
5	Castle Gate	Upper Cretaceous	1000×1000×1000	2.25	0.25	High
6	Kirby	Cretaceous	1000×1000×1000	2.25	0.22	Low
7	Leopard	Paleozoic	1000×1000×1000	2.25	0.20	High
8	Parker	Paleozoic	1000×1000×1000	2.25	0.14	Low
9	Zebra A	Cambrian	600×600×900	2.00	0.16	Low
10	Zebra B	Cambrian	600×600×900	2.00	0.15	Low

11	Bandera Gray A	Upper Carboniferous	600×600×900	2.00	0.14	Low
12	Bandera Gray B	Upper Carboniferous	600×600×900	1.97	0.19	Low

Table 4. Information of carbonate rocks.

No.	Name	Formation	Size	Resolution (μm)	Porosity	Permeability
1	Estaillades	Tertiary	1000×1000×1000	3.1	0.12	Intermediate
2	Grosmont	Upper Devonian	1000×1000×1000	2.02	0.19	Intermediate
3	Austin Chalk	upper Cretaceous	640×670×950	0.70	0.31	Low
4	SAVII2	Middle Jurassic	1000×1000×1600	3.8	0.24	Intermediate
5	Indiana	Lower Carboniferous	1520×1520×3522	2.68	0.22	Intermediate
6	Middle East	-	1520×1520×4100	2.68	0.19	Intermediate
7	Leuders A	Cretaceous	600×600×900	1.03	0.15	Low
8	Leuders B	Cretaceous	600×600×900	1.03	0.18	Low
9	Leuders C	Cretaceous	600×600×900	2.00	0.29	Low
10	Bonne Terre A	Cambrian	600×600×900	1.03	0.17	Low
11	Bonne Terre B	Cambrian	600×600×900	1.02	0.10	Low
12	Bonne Terre C	Cambrian	600×600×900	2.00	0.19	Low

Acknowledgements

We acknowledge Shell for financial support and for providing the digital rock images. This study has mostly been performed using the Sherlock cluster at Stanford University. We are grateful to Stanford University and the Stanford Research Computing Center for providing computational resources and support in this research. We acknowledge the sponsors of the Stanford Center for Earth Resources Forecasting (SCERF) and support from Prof. Steve Graham, the Dean of the

Stanford School of Earth, Energy and Environmental Sciences. The authors also would like to thank Math2Market for providing the GeoDict software at a discount and technical support, the Pore-Scale Modelling and Imaging Group at Imperial College London for sharing the poreFoam codes, and the Digital Rocks Portal (https://www.digitalrocksportal.org) for providing the open source data.

Data Availability Statement

The code is freely available on the GitHub repository (https://github.com/theanswer003/PermNet) (Liu, 2022a). The datasets are available from http://dx.doi.org/10.17632/nv5dhfj86t.1 (Liu, 2022b).

References

- Ahmad, R., Liu, M., Ortiz M., Mukerji, T., & Cai W. (2022). Computation of effective elastic moduli of rocks using hierarchical homogenization. *arXiv preprint* arXiv: 2208.02320.
- Alqahtani, N., Mostaghimi, P., & Armstrong, R. (2021). A Multi-Resolution Complex Carbonates Micro-CT Dataset (MRCCM). [Dataset]. https://www.digitalrocksportal.org/projects/362
- Andrä, H., Combaret, N., Dvorkin, J., Glatt, E., Han, J., Kabel, M., Keehm, Y., Krzikalla, F., Lee, M., Madonna, C., & Marsh, M. (2013a). Digital rock physics benchmarks—Part I: Imaging and segmentation. *Computers & Geosciences, 50*, 25-32.
- Andrä, H., Combaret, N., Dvorkin, J., Glatt, E., Han, J., Kabel, M., Keehm, Y., Krzikalla, F., Lee, M., Madonna, C., & Marsh, M. (2013b). Digital rock physics benchmarks—Part II: Computing effective properties. *Computers & Geosciences, 50*, 33-43.
- Balhoff, M.T., Thomas, S.G., & Wheeler, M.F. (2008). Mortar coupling and upscaling of pore-scale models. *Computational Geosciences, 12*(1), 15-27.
- Blunt, M.J., Bijeljic, B., Dong, H., Gharbi, O., Iglauer, S., Mostaghimi, P., Paluszny, A., & Pentland, C. (2013). Pore-scale imaging and modelling. *Advances in Water resources, 51*, 197-216.
- Brinkman, H.C. (1949). A calculation of the viscous force exerted by a flowing fluid on a dense swarm of particles. *Flow, Turbulence and Combustion, 1*(1), pp.27-34.
- Bultreys, T. (2016). Estaillades Carbonate #2. [Dataset]. https://www.digitalrocksportal.org/projects/58
- Carman, P.C. (1937). Fluid flow through granular beds. *Trans.-Inst. Chem. Eng., 15*, 150-166.
- Chan, T.F., & Mathew, T.P. (1994). Domain decomposition algorithms. *Acta numerica, 3*, 61-143.
- Cui, R., Cao, D., Liu, Q., Zhu, Z., & Jia, Y. (2021). VP and VS prediction from digital rock images using a combination of U-Net and convolutional neural networks. *Geophysics, 86*(1), MR27-MR37.
- Da Wang, Y., Chung, T., Armstrong, R.T., McClure, J.E., & Mostaghimi, P. (2019). Computations of permeability of large rock images by dual grid domain decomposition. *Advances in water resources, 126*, 1-14.

- Dosovitskiy, A., Beyer, L., Kolesnikov, A., Weissenborn, D., Zhai, X., Unterthiner, T., Dehghani, M., Minderer, M., Heigold, G., Gelly, S., & Uszkoreit, J. (2020). An image is worth 16x16 words: Transformers for image recognition at scale. *arXiv preprint* arXiv:2010.11929.
- Gropp, W.D., & Keyes, D.E. (1992). Domain decomposition methods in computational fluid dynamics. *International journal for numerical methods in fluids, 14*(2), pp.147-165.
- He, K., Zhang, X., Ren, S., & Sun, J. (2016). Deep residual learning for image recognition. In *Proceedings of the IEEE conference on computer vision and pattern recognition* (pp. 770-778).
- Huang, R., Herring, A.L., & Sheppard, A. (2021). Effect of Saturation and Image Resolution on Representative Elementary Volume and Topological Quantification: An Experimental Study on Bentheimer Sandstone Using Micro-CT. *Transport in Porous Media, 137*(3), pp.489-518.
- Karimpouli, S., & Tahmasebi, P. (2019). Image-based velocity estimation of rock using convolutional neural networks. *Neural Networks, 111*, 89-97.
- Kashefi, A., & Mukerji, T. (2021). Point-cloud deep learning of porous media for permeability prediction. *Physics of Fluids, 33*(9), 097109.
- Keehm, Y., Mukerji, T., & Nur, A. (2001). Computational rock physics at the pore scale: Transport properties and diagenesis in realistic pore geometries. *The Leading Edge, 20*(2), 180-183.
- Keehm, Y., Mukerji, T., & Nur, A. (2004). Permeability prediction from thin sections: 3D reconstruction and Lattice-Boltzmann flow simulation. *Geophysical Research Letters, 31*(4).
- Kozeny, J. (1927). Über kapillare Leitung des Wassers im Boden. *Sitzungsber Akad. Wiss., Wien., 136*(2a), 271-306.
- Linden, S., Wiegmann, A., & Hagen, H. (2015). The LIR space partitioning system applied to the Stokes equations. *Graphical Models, 82*, 58-66.
- Lindquist, S.J. (1988). Practical characterization of eolian reservoirs for development: Nugget Sandstone, Utah—Wyoming thrust belt. *Sedimentary Geology, 56*(1-4), 315-339.

- Liu, M. (2022a). Digital rock dataset for use in machine learning research of permeability prediction. [Dataset]. Mendeley Data, V1, doi: 10.17632/nv5dhfj86t.1.
- Liu, M. (2022b). Hierarchical homogenization with deep-learning-based surrogate model for rapid estimation of effective permeability from digital rocks. [Source code]. https://github.com/theanswer003/PermNet
- Liu, M., & Mukerji, T. (2022). Multiscale fusion of digital rock images based on deep generative adversarial networks. *Geophysical Research Letters*, e2022GL098342.
- Menke, H.P., Maes, J., & Geiger, S. (2021). Upscaling the porosity–permeability relationship of a microporous carbonate for Darcy-scale flow with machine learning. *Scientific reports, 11*(1), pp.1-10.
- Nath, F., Salvati, P.E., Mokhtari, M., Seibi, A., & Hayatdavoudi, A. (2017). Observation of fracture growth in laminated sandstone and carbonate rock samples under Brazilian testing conditions using digital image correlation technique. *In SPE Eastern Regional Meeting. OnePetro*.
- Neumann, R., Andreeta, M., & Lucas-Oliveira, E. (2020). 11 Sandstones: raw, filtered and segmented data. [Dataset]. https://www.digitalrocksportal.org/projects/317.
- Pranter, M.J. & Sommer, N.K. (2011). Static connectivity of fluvial sandstones in a lower coastal-plain setting: An example from the Upper Cretaceous lower Williams Fork Formation, Piceance Basin, Colorado. *AAPG bulletin, 95*(6), 899-923.
- Rabbani, A., Babaei, M., Shams, R., Da Wang, Y., & Chung, T. (2020). DeePore: a deep learning workflow for rapid and comprehensive characterization of porous materials. *Advances in Water Resources, 146*, 103787.
- Raeini, A.Q., Blunt, M.J., & Bijeljic, B. (2012). Modelling two-phase flow in porous media at the pore scale using the volume-of-fluid method. *Journal of Computational Physics, 231*(17), 5653-5668.
- Santos, J.E., Xu, D., Jo, H., Landry, C.J., Prodanović, M., & Pyrcz, M.J. (2020). PoreFlow-Net: A 3D convolutional neural network to predict fluid flow through porous media. *Advances in Water Resources, 138*, 103539.

- Santos, J.E., Yin, Y., Jo, H., Pan, W., Kang, Q., Viswanathan, H.S., Prodanović, M., Pyrcz, M.J., & Lubbers, N. (2021). Computationally efficient multiscale neural networks applied to fluid flow in complex 3D porous media. *Transport in porous media*, *140*(1), 241-272.
- Saxena, N., Hofmann, R., Alpak, F.O., Berg, S., Dietderich, J., Agarwal, U., Tandon, K., Hunter, S., Freeman, J., & Wilson, O.B. (2017). References and benchmarks for pore-scale flow simulated using micro-CT images of porous media and digital rocks. *Advances in Water Resources*, *109*, 211-235.
- Shabro, V., Torres-Verdín, C., Javadpour, F., & Sepehrnoori, K. (2012). Finite-difference approximation for fluid-flow simulation and calculation of permeability in porous media. *Transport in porous media*, *94*(3), 775-793.
- Simonyan, K., & Zisserman, A. (2014). Very deep convolutional networks for large-scale image recognition. *arXiv preprint arXiv*:1409.1556.
- Vianna, R.S., Cunha, A.M., Azeredo, R.B., Leiderman, R., & Pereira, A. (2020). Computing Effective Permeability of Porous Media with FEM and Micro-CT: An Educational Approach. *Fluids*, *5*(1), 16.